

Accepted Manuscript

Synthesis and biological evaluation of pyridazinone derivatives as potential anti-inflammatory agents

Chantal Barberot, Aurélie Moniot, Ingrid Allart-Simon, Laurette Malleret, Tatiana Yegorova, Marie Laronze-Cochard, Abderrazzaq Bentaher, Maurice Médebielle, Jean-Philippe Bouillon, Eric Hénon, Janos Sapi, Frédéric Velard, Stéphane Gérard

PII: S0223-5234(18)30048-5

DOI: [10.1016/j.ejmech.2018.01.035](https://doi.org/10.1016/j.ejmech.2018.01.035)

Reference: EJMECH 10112

To appear in: *European Journal of Medicinal Chemistry*

Received Date: 11 October 2017

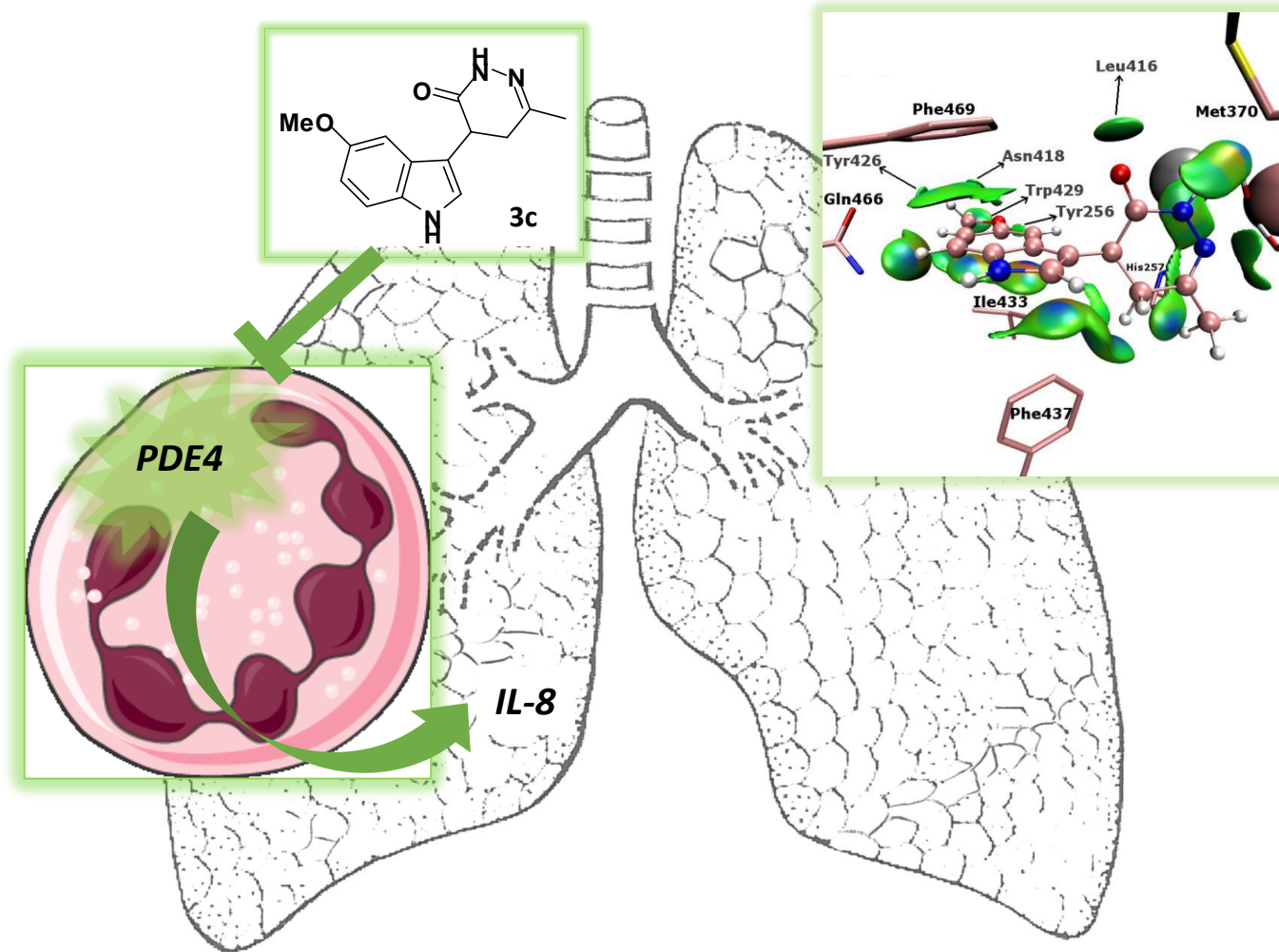
Revised Date: 10 January 2018

Accepted Date: 11 January 2018

Please cite this article as: C. Barberot, Auré. Moniot, I. Allart-Simon, L. Malleret, T. Yegorova, M. Laronze-Cochard, A. Bentaher, M. Médebielle, J.-P. Bouillon, E. Hénon, J. Sapi, Frée. Velard, Sté. Gérard, Synthesis and biological evaluation of pyridazinone derivatives as potential anti-inflammatory agents, *European Journal of Medicinal Chemistry* (2018), doi: 10.1016/j.ejmech.2018.01.035.

This is a PDF file of an unedited manuscript that has been accepted for publication. As a service to our customers we are providing this early version of the manuscript. The manuscript will undergo copyediting, typesetting, and review of the resulting proof before it is published in its final form. Please note that during the production process errors may be discovered which could affect the content, and all legal disclaimers that apply to the journal pertain.





Synthesis and Biological Evaluation of Pyridazinone derivatives as Potential Anti-inflammatory Agents

Chantal Barberot,^a Aurélie Moniot,^b Ingrid Allart-Simon,^a Laurette Malleret,^c Tatiana Yegorova,^d Marie Laronze-Cochard,^a Abderrazzaq Bentaher,^c Maurice Médebielle,^e Jean-Philippe Bouillon,^d Eric Hénon,^a Janos Sapi,^a Frédéric Velard^b and Stéphane Gérard^{*a}

a) Université de Reims Champagne-Ardenne, Institut de Chimie Moléculaire de Reims (ICMR), UMR CNRS 7312, UFR Sciences, Moulin de la housse and UFR Pharmacie, 51 rue Cognacq-Jay, 51096 Reims, France.

b) Université de Reims-Champagne-Ardenne, EA 4691 Biomatériaux & Inflammation en site OSseux (BIOS), UFR Pharmacie and UFR Odontologie, 51 rue Cognacq-Jay, 51096 Reims, France

c) Centre International de Recherche en Infectiologie (CIRI), EA7426, Faculté de Médecine Lyon-Sud, 165 chemin du Grand Revoyet, 69921 Oullins, France

d) Normandie Univ, INSA Rouen, UNIROUEN, CNRS, COBRA (UMR 6014), 76000 Rouen, France

e) Univ Lyon, Université Lyon 1, CNRS, INSA, CPE-Lyon, ICBMS, UMR 5246, 43 bd du 11 Novembre 1918, 69622 Villeurbanne, France

Abstract : Cyclic nucleotide phosphodiesterase type 4 (PDE4), that controls intracellular level of cyclic nucleotide cAMP, has aroused scientific attention as a suitable target for anti-inflammatory therapy in respiratory diseases. Here we describe the development of two families of pyridazinone derivatives as potential PDE4 inhibitors and their evaluation as anti-inflammatory agents. Among these derivatives, 4,5-dihydropyridazinone representatives possess promising activity, selectivity towards PDE4 isoenzymes and are able to reduce IL-8 production by human primary polymorphonuclear cells.

Keywords : Pyridazinone - phosphodiesterase inhibitors - anti-inflammatory - PDE4

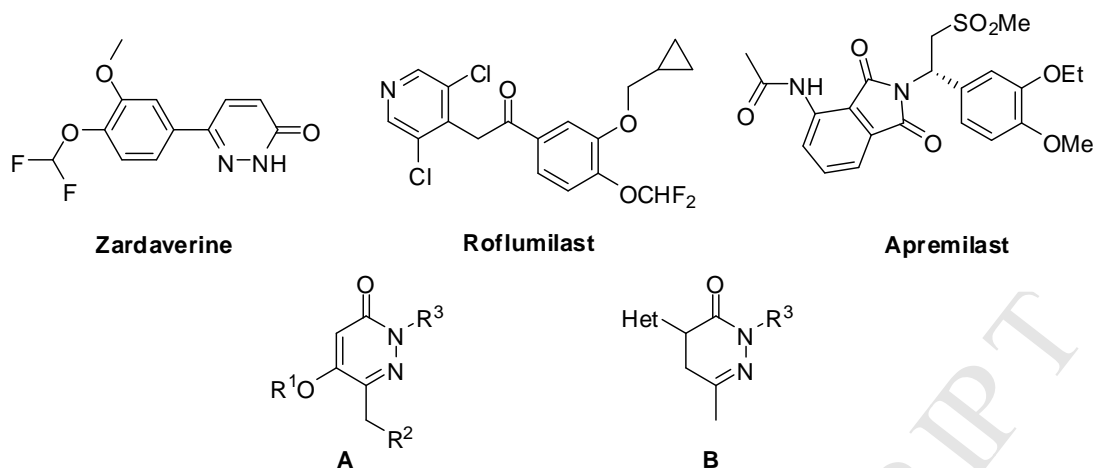
Introduction

The chemistry of pyridazinones has been an interesting field of study since decades and this six membered ring has then become a scaffold of choice for the development of potential drug-candidates [1]. Thus these nitrogen-rich heterocyclic derivatives have been known to exhibit many pharmacological actions against ulcer [2] or cardiovascular diseases [3] or as anti-proliferative agents [4,5]. Development of new pyridazinone-based analgesic and anti-inflammatory derivatives acting as selective COX-2 inhibitors was recently described as well as the design of pyrazolo pyrimidopyridazinones for the treatment of erectile dysfunction [6,7]. An identified therapeutic application of such scaffold is its anti-inflammatory activity by targeting phosphodiesterases and our interest in this heterocyclic system stems from the pyridazinone type PDE3/PDE4 dual inhibitor, Zardaverine (Scheme 1),

which reached clinical development for the treatment of chronic obstructive pulmonary disease (COPD) [8].

In recent years, phosphodiesterases, a superfamily of eleven intracellular enzymes, responsible for the hydrolysis of cyclic adenosine and/or guanosine monophosphate (intracellular second messengers facilitating the action of hormones and inflammatory mediators) have emerged as new therapeutic targets with special attention given to phosphodiesterase type-4 (PDE4). From a biological point of view, PDE4 is the predominant isoenzyme found in inflammatory and immunomodulatory cells and is overexpressed in many airway cells such as epithelial and immune cells including neutrophils, T-cells, and macrophages [9]. By its inhibition both airway smooth muscle relaxation and inflammatory mediator release can be managed, therefore PDE4 may be considered as a valuable biological target for the treatment of inflammatory or pulmonary diseases [10]. More recently PDE4 inhibition also demonstrated positive effects against aberrant immune response diseases such as atopic dermatitis, rheumatoid arthritis or psoriasis or in the modulation of metabolic disorders such as obesity or type 2 diabetes [11]. Although a large number of PDE4 inhibitors have been clinically evaluated, the use of first-generation has been hampered by cardiac and emetic mechanism-associated side effects. Second-generation selective inhibitors like Roflumilast and Apremilast were generally better-tolerated and are currently approved for the treatment of COPD and plaque psoriasis, respectively (Scheme 1) [12,13]. Additionally, Barreiro *et al.* also showed the assessment of *N*-acyl hydrazones (possessing bioisosteric relationship with the pyridazinone ring) as conformationally constrained PDE4 inhibitors to limit the inflammatory response observed in pulmonary diseases [14] while biphenyl pyridazinone derivatives were recently developed by Gracia *et al.* as inhaled PDE4 inhibitors [15].

In continuation of our efforts to develop selective inhibitors of PDE4 for the treatment of respiratory diseases possessing fewer side effects than marketed compounds [16], we describe herein the synthesis of the first representatives of two new classes of pyridazinone derivatives (structures **A** and **B**, scheme 1) and their evaluation as potential anti-inflammatory agents. As dialkoxyphenyl containing molecules have shown to be selective inhibitors of PDE4 [17], probably by formation of hydrogen bonds with a glutamine residue at the back of the catalytic site [18], we chose to introduce alkoxy or catechol moieties on the pyridazinone scaffold of compounds of **A** family. Simultaneously the design of **B** family was based on the work of Pieretti and Dal Piaz [19,20]. They developed constrained pyridazinones fused with heterocyclic nucleus (thiophene or isoxazole) as possible anti-inflammatory agents. In



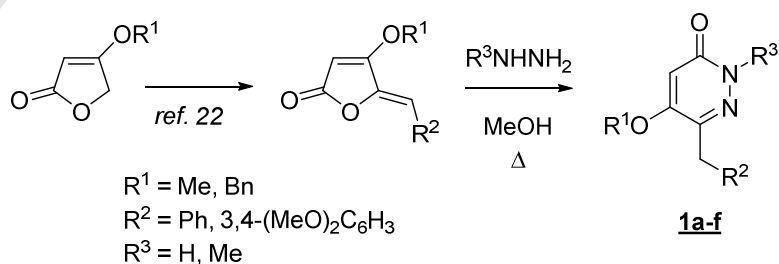
Scheme 1: Structures of Zardaverine, approved drugs Roflumilast and Apremilast and the two targeted families

complementary manner Timmerman focused his work on dihydropyridazinones possessing *cis*-fused cyclohexane ring as PDE4 inhibitors [21]. So, in our derivatives, we would like to introduce a degree of conformational freedom between pyridazinone scaffold and heterocyclic moiety in order to study if these constrained conformations can influence potency and selectivity over PDE4. Preparation of the targeted compounds was efficiently achieved by using two flexible stepwise procedures.

Results and discussions

Chemistry

First representatives of pyridazinone derivatives of **A** family were obtained by condensation of hydrazines onto 5-arylidene tetronates intermediates prepared from the corresponding methyl or benzyl tetronates by our aldolisation/deshydration one pot sequence (Scheme 2) [22]. This approach furnished pyridazinones bearing 5-alkoxy substituent **1a-f** in moderate to good yields (Table 1).

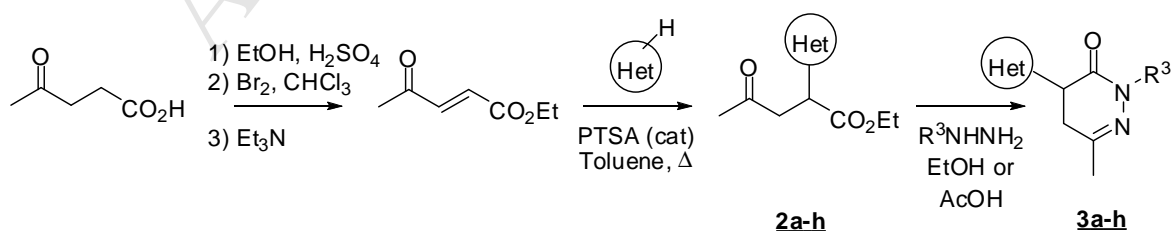


Scheme 2: Synthesis of 5-alkoxy-pyridazinones

Entry	Compound	R ¹	R ²	R ³	Yield (%)
1	1a	Me	Ph	H	52
2	1b	Me	Ph	Me	41
3	1c	Bn	Ph	H	27
4	1d	Bn	Ph	Me	50
5	1e	Bn	3,4-(MeO) ₂ C ₆ H ₃	H	88
6	1f	Bn	3,4-(MeO) ₂ C ₆ H ₃	Me	59

Table 1: Isolated yields of 5-alkoxy-pyridazinones

We then turn our attention to the preparation of compounds of **B** family. These pyridazinone derivatives were obtained by a three-step sequence starting from levulinic acid (Scheme 3) [23]. After preparation of the corresponding α,β -unsaturated levulinate [24], regioselective introduction of the heterocyclic system was carried out by Friedel-Crafts type reaction leading to intermediate compounds **2a-h** [25]. Both aliphatic and aromatic heterocycles were used. As shown in the Table 2, formation of the corresponding adduct proceeded in about 48h in moderate to good yields. Different indoles as well as benzotriazole could be used in this condensation. Moreover, the use of C-3 substituted indole offered the possibility to obtain condensation in the less reactive 2 position (entry 4). Addition product of morpholine and *N*-methylpiperazine could also be obtained in satisfactory yields while dimer adduct of levulinate was the major product of the reaction with piperazine (entry 7). Subsequent condensation of intermediates **2a-h** with hydrazine or methylhydrazine led to the formation of the desired 4,5-dihydropyridazinones **3a-h** functionalized by a heterocyclic moiety in position 4 with good yields.



Scheme 3: Synthesis of 4,5-dihydropyridazinones bearing heterocycle in position 4

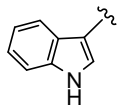
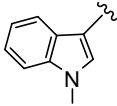
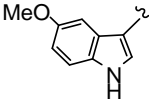
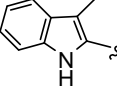
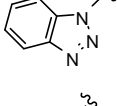
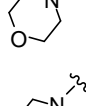
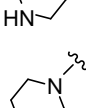
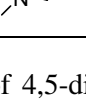
Entry	Heterocycle (Het)	Compound (Yield ^a (%))	R ³	Compound (Yield ^a (%))
1		2a (53 %)	H	3a (61 %)
			Me	3i (81 %)
2		2b (56 %)	H	3b (53 %)
3		2c (55 %)	H	3c (76 %)
4		2d (69 %)	H	3d (54 %)
5		2e (65 %)	H	3e (15 %)
6		2f (76 %)	H	3f (45 %)
			Me	3g (48 %)
7		2g (38 %) ^b	H	/
8		2h (57 %)	H	3h (85 %)

Table 2: Synthesis of 4,5-dihydropyridazinones bearing heterocycle in position 4 [note: a) yield of isolated product; b) dimer product with traces of monomer (see experimental section)]

PDE4 inhibition

All synthesized compounds were then screened for their potential inhibitory activity on PDE4 (Table 3). The evaluation approach, based on a "non radioactive" assay recently developed in our laboratory [16a], could be directly applied for the selection of privileged pyridazinone derivatives during "hit detection" step. Results were expressed as inhibition percentage of PDE4 at an initial concentration of 500 μ M. For the most potent hits, preliminary PDE selectivity (PDE1 isoform) and evaluated IC_{50} are also collected in Table 3.

Preliminary results of *in-vitro* evaluations performed on the two series of molecules showed better activity of **B** family members rather than 5-alkoxy-pyridazinones **A** although

introduction of catechol moiety slightly increased potency of this pyridazinone scaffold (entries

Entry	Compound	PDE4 ^{a,b} (%)	PDE1 ^{a,b} (%)	IC ₅₀ ^{b,c} (μM)
1	1a	43	nd	nd
2	1b	53	nd	nd
3	1c	39	nd	nd
4	1d	46	nd	nd
5	1e	67	nd	nd
6	1f	61	nd	nd
7	3a	87	23	32
8	3b	59	nd	nd
9	3c	91	9	23
10	3d	89	22	nd
11	3e	21	nd	nd
12	3f	43	31	nd
13	3g	94	34	35
14	3h	38	nd	nd
15	3i	53	nd	nd
16	Zardaverine	74 ^d	25 ^d	2
17	IBMX	28 ^d	92 ^d	38

Table 3: Biochemical evaluation of pyridazinones as PDEs inhibitors [note: a) inhibition at initial concentration of 500 μM; b) mean of two or three experiments, each performed in triplicate, protocols are given in the experimental section; c) IC₅₀ on PDE4 evaluated by non-linear regression; d) inhibition at 40 μM; nd: not determined]

5 and 6). Indeed, most of 4,5-dihydropyridazinones bearing heterocycle in position 4 possess significant inhibitory activity (IC₅₀ = 20-40 μM for the best compounds) and promising selectivity profile for PDE4 (*vs* PDE1) compared to reference substances: Zardaverine (IC₅₀ = 2 μM and 25% PDE1 inhibition at 40 μM in our conditions) and non-specific PDE inhibitor 3-isobutyl-1-methylxanthine (IBMX).

First *in-vitro* results obtained on the **B** family showed that all of 4,5-dihydropyridazinones bearing indole moiety on the 4-position of the heterocyclic scaffold exhibited quite similar activities and selectivities with interesting percentages of PDE4 inhibition. Our attention turned to the *N*-substituent of the indole and pyridazinone rings. It was determined that these hydrogen bond donor functions were optimal for the affinity for PDE4 in so far as *N*-methyl derivatives **3b** and **3i** appeared about 1.5-fold less potent than the

corresponding analogue **3a**. In this family, replacing indole by benzotriazole drastically reduced the affinity for PDE4 receptors, thus **3e** was found to be practically inactive at screening concentration. Interestingly, contrary to our initial expectation, decreasing hydrophobic character of the heterocyclic moiety (**3g** vs **3c**) slightly modified the inhibitory effect but might have an impact on selectivity.

Comparison of these different pharmacological data showed that the more active pyridazinone is the compound **3c** functionalized with 5-methoxyindole moiety possessing 91% of inhibition of PDE4 at 500 μM and IC_{50} about 20 μM . However this compound remained about 10-fold less active than our reference compound Zardaverine but displayed a better selectivity towards PDE1. This compound **3c**, and its analog **3a**, were selected for further investigations.

Molecular modeling

After screening and hit-detection a challenging task is to address the binding mode of our ligands. The protein structure was prepared from the available PDB structure 1MKD (PDE4D isoform, see computational details section) and molecular docking simulations were performed on the most active compounds. 3D representations of interactions regions are reported for two of them on Figures 1 and 2. As pointed out by a previous study [26], browsing the first ranked poses of all compounds shows two key features: (1) hydrogen bonding (HB) with Gln466 and (2) van der Waals (vdW) interactions on both sides of the ligand fitting an oblong cavity formed by residues Ile433, Phe437 and Phe469. This is in line with the X-ray pose of the Zardevarine in PDE4 [27]. Accordingly, in our 4,5-dihydropyridazinone **3a** (pose not reported here), the planar indole moiety is more appropriate than the pyridazinone motif to fit in the hydrophobic pocket, as observed in the top-ranked pose obtained ($\Delta_r G^0 = -8.7 \text{ kcal.mol}^{-1}$). However, in that case, no HB can be observed between Gln466 and the indole part (HB-donor). Similarly (see Figure 1a), the best pose obtained for **3c** ($\Delta_r G^0 = -8.7 \text{ kcal.mol}^{-1}$) also puts the planar indole group in the oblong hydrophobic pocket of PDE4. But the presence of the methoxy group in **3c** allows for additional interactions, either vdW contacts with residues Trp429 and Asn418 (Figure 1b, pose 1), or even HB with Gln466 (Figure 1c, pose 2). In that case, the methyl group can also interact with Met454 as clearly revealed by the corresponding weak-interaction iso-surfaces. Although the Vina scores for **3a** and **3c** best poses are identical, the additional conformational possibilities provided by

the methoxy group could explain the better affinity observed for **3c**. On the other hand, the pyridazinone motif interacts with Met370 and can also establish HB with His257 as illustrated on Figure 1c. It is worth noting that the ligand doesn't interact directly with the two metal ions but rather with the coordinated water molecules. On Figure 1a, the atoms are colored according to their contribution to the interaction (NCI/IGM analysis [28], a new methodology derived from NCI). This analysis clearly shows that the indole moiety primarily contributes to the interactions in this complex. Finally, a pose is presented on Figure 1d where the pyridazinone moiety fills the oblong hydrophobic pocket (-7.6 kcal.mol⁻¹, pose 5). Obviously it is not a favorable situation because the strong HB interaction with the key residue Gln466 is lost in that case.

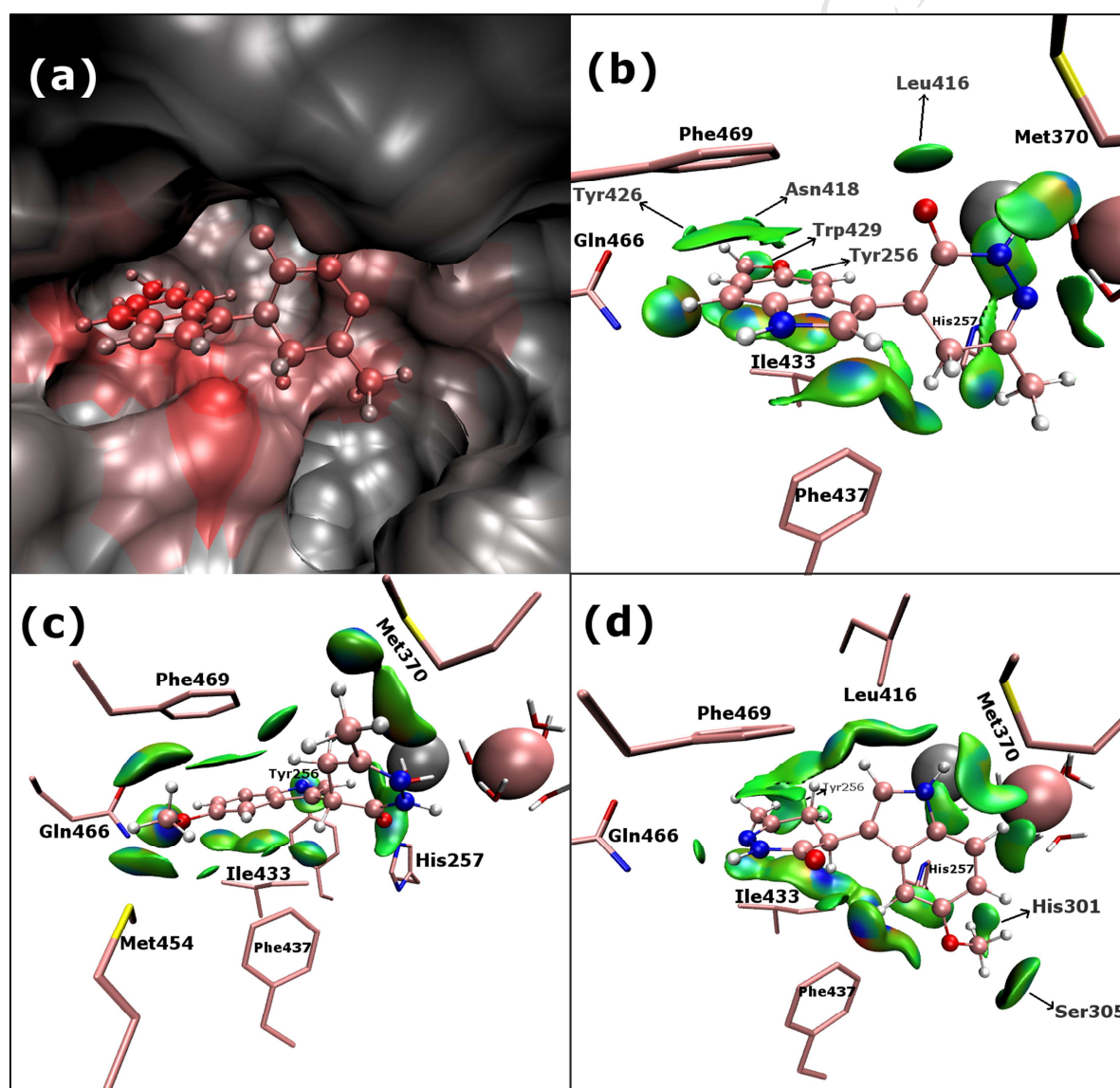


Figure 1. Analysis of non-covalent interactions (NCI) between PDE4 and **3c**, using the NCI/IGM method derived from the NCI tool; poses obtained with software Autodock-Vina [28]; (a) atoms of the complex colored according to their contribution to the interaction iso-surfaces described in panel b; a grey-to-red color scheme is used in the range 0 to 2.89, with grey: no contribution to the NCI and red:

largest relative contribution to the NCI; (b) top-ranked pose: $-8.7 \text{ kcal.mol}^{-1}$; (c) second pose: $-7.8 \text{ kcal.mol}^{-1}$; (d) fifth pose: $-7.6 \text{ kcal.mol}^{-1}$; every iso-surface has been obtained using $\delta g^{\text{inter}} = 0.007 \text{ a.u.}$ and is colored according to the BGR scheme over the signed electron density range $-0.05 < \text{sign}(\lambda_2)\rho < 0.05 \text{ a.u.}$

In addition we would like to understand the pharmacological data obtained for 4,5-dihydropyridazinone **3g**. This complementary work indicates a different positioning of this compound (Fig 2). Here, the best pose ($-6.6 \text{ kcal.mol}^{-1}$, pose 1) displays the non-planar pyridazinone motif filling the hydrophobic pocket. The interaction iso-surfaces reveal a substantial HB interaction with Gln466. However, according to the atomic analysis of the interactions (Figure 2a), the oxygen and nitrogen atoms of the heterocyclic moiety hardly contribute to the interactions. The ligand affinity and lower selectivity observed for this species could be explained by this less effective binding mode. Finally, it can be noted that our compounds are too small to reach an additional hydrophobic channel present in the active site (at the bottom right of Figures 1a and 2a). This theoretical study establishes a first interesting basis for compound comparison and points out key features for efficient binding. Further investigations (molecular dynamics for instance) might provide better insight in the observed affinities and selectivities by introducing the protein flexibility into the simulations. However, theoretical computations are nonetheless limited and cannot capture the overall complex biological response.

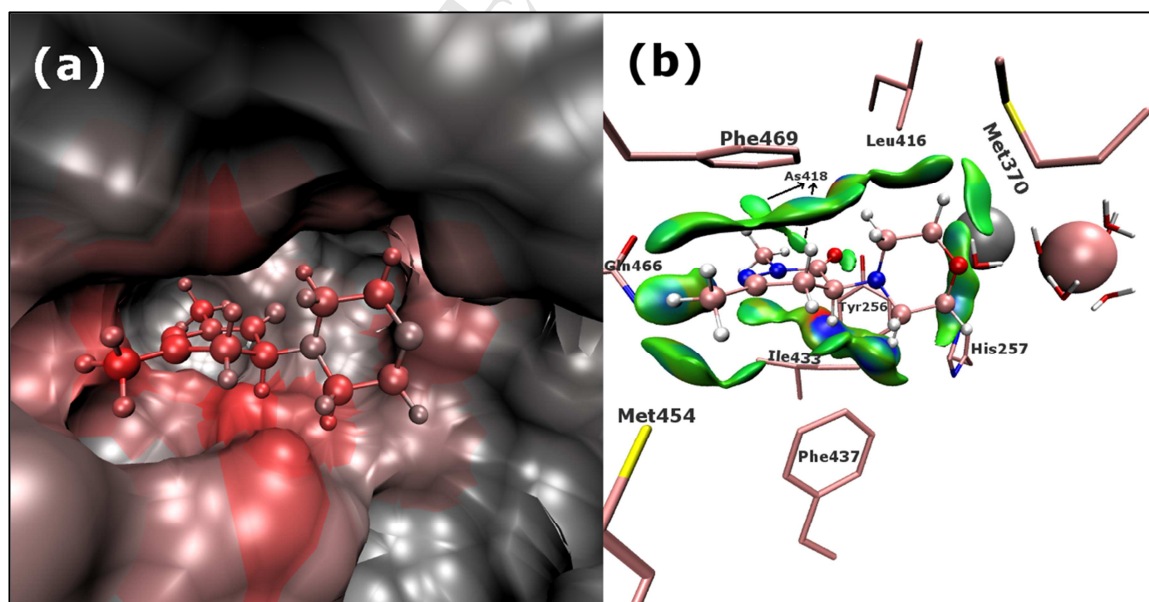


Figure 2. Analysis of non-covalent interactions (NCI) between PDE4 and **3g**, using the NCI/IGM method derived from the NCI tool; poses obtained with software Autodock-Vina; (a) atoms of the complex colored according to their contribution to the interaction iso-surfaces described in panel b; a grey-to-red color scheme is used in the range 0 to 2.89, with grey: no contribution to the NCI and red: largest relative contribution to the NCI; (b) top-ranked pose: $-6.6 \text{ kcal.mol}^{-1}$; iso-surfaces have been

obtained using $\delta g^{\text{inter}} = 0.007$ a.u. and are colored according to the BGR scheme over the electron density range $-0.05 < \text{sign}(\lambda_2)\rho < 0.05$ a.u.

Biology

The two selected compounds **3a** and **3c** were then evaluated for their *in vitro* cellular activity in the blockade of chemokine production. We first evaluated the toxicity of PDE4 inhibitors in pro-inflammatory environment by measuring LDH release by human polymorphonuclear leukocytes (PMNs) (Figure 3). Test compounds were dissolved in culture media containing 0.5% DMSO with no evidence of lack of solubility. After four hours of culture in presence of lipopolysaccharide (LPS), PMNs supernatants showed a slight but significant increase (20% increase of median value) in LDH activity which was not retrieved in presence of PDE4 inhibitors as compared to the control condition. Such a tolerance toward PDE4 inhibitors was already suggested in studies demonstrating their anti-inflammatory potential against LPS-induced immune cells activation [29].

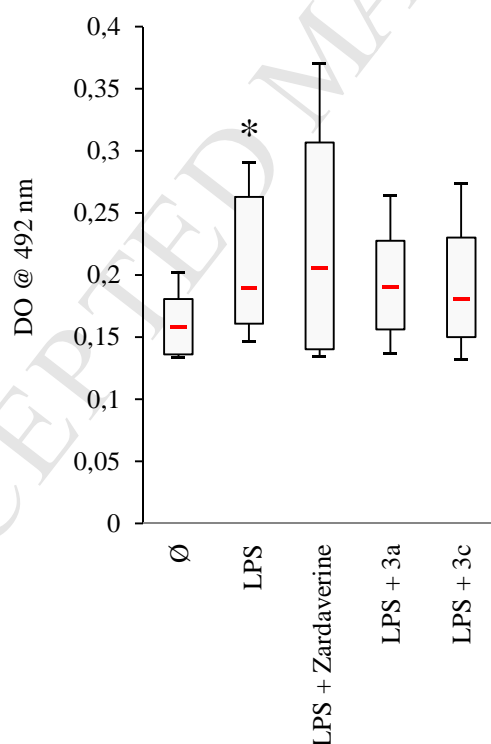


Figure 3: Cell death evaluation by measurement of LDH activity in human PMNs culture supernatants (n=10). Red bar represents median value. Black bars represent 1st and 9th decile and limits of rectangles represent 1st and 3rd quartile. * $p < 0.05$ when compared with non-stimulated (control) cells.

We then measured the inhibition of IL-8 production in the PMNs to give a translation between the *in vitro* enzymatic potency and cell-based assay. IL-8 production by PMNs in response to pro-inflammatory molecules is a very well described phenomenon. Here we confirmed in our model that LPS is able to induce an increased IL-8 secretion by human primary PMNs (3 fold increase of median value). Of interest, we highlighted that PDE4 inhibitors **3a** and **3c** were able to statistically reduce this IL-8 production in 7 and 9 of 10 donors respectively (10% and 15% reduction of median value) whereas Zardaverine failed to demonstrate such an effect (Figure 4).

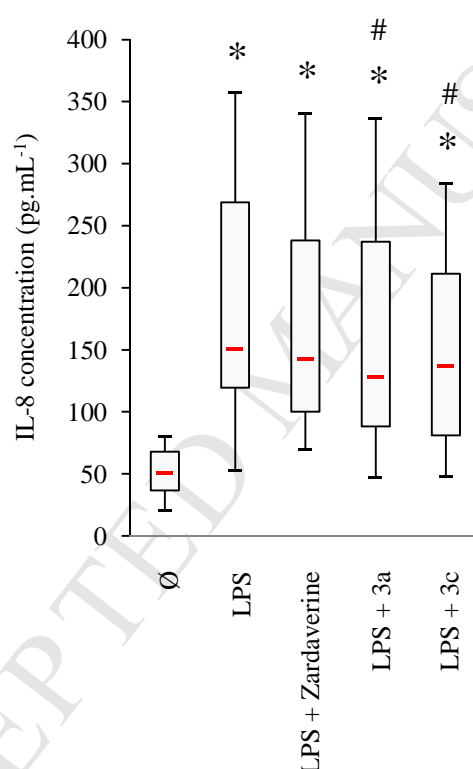


Figure 4: ELISA measurements of IL-8 concentrations in unexposed or LPS-exposed cell supernatants after 4 h. Red bar represents median value. Black bars represent 1st and 9th decile and limits of rectangles represent 1st and 3rd quartile. n=10 independent experiments. * $p < 0.05$ when compared with nonstimulated (control) cells. # $p < 0.05$ when compared with LPS-stimulated cells. n=10 independent experiments.

As IL-8 is both a potent activator and also a powerful chemoattractant for PMNs, we next assessed the effect of anti-PDE4 compounds on PMNs migratory abilities. Our data indicated that rhIL-8 induced an increased number of migrating PMNs as compared to spontaneous migration in basal conditions (Figure 5). PMNs ability to follow chemotactic gradient of IL-8 was impaired with all anti PDE4 compounds. In addition, when cells were co-incubated with Zardaverine the chemotaxis is statistically reduced versus rhIL-8. In the

same way, compound **3a** tended to decrease the migrating cell number (median value decreased by 50%) but failed to reach statistical threshold. These data are consistent with previous studies highlighting neutrophils activation and chemotaxis impairments after PDE4 inhibition independently of the initial stimulus [30,31].

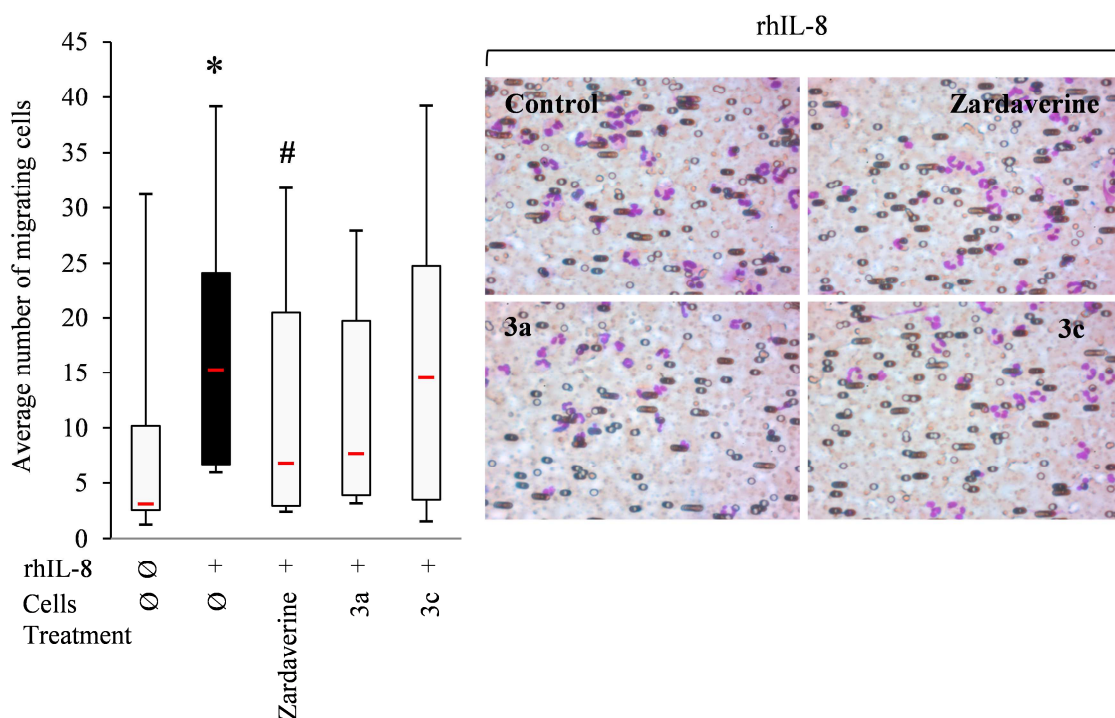


Figure 5: Boyden chamber chemotaxis assay. PMNs were seeded at 10^6 per mL in the upper wells and allowed to migrate for 45 min against rhIL-8 200 ng.mL^{-1} (lower wells). Migrated cells through the membrane were counted after staining. Red bar represents median value. Black bars represent 1st and 9th decile and limits of rectangles represent 1st and 3rd quartile. Shown are representative photographs of MGG staining. Scale bar = 25 μm . Objective x40, Zeiss Axiovert 200M. n=8 independent experiments. * $p < 0.05$ when compared with basal migrating cells. # $p < 0.05$ when compared with rhIL-8-chemoattracted cells.

Conclusion

In conclusion, two new families of molecules possessing pyridazinone scaffold were obtained in few steps from 5-arylidene tetronates or levulinic acid derivative and were evaluated for their potential anti-inflammatory activity. After screening and hit-detection a theoretical study (NCI/IGM method) helped us to rationalize the binding mode of our ligands. Among the prepared compounds, 4,5-dihydropyridazinones **3a** and **3c** bearing an heterocyclic moiety (indole and 5'-methoxyindole, respectively) on the 4-position exhibited PDE4 selectivity vs PDE1 and interesting activity ($IC_{50} \sim 20$ and $30 \mu\text{M}$, respectively). Of

physiologic relevance, identified hits **3a** and **3c** possess neither cytotoxic effect nor abnormal pro-inflammatory role on polymorphonuclear leukocytes cells as judged by LDH cytotoxicity assay and we highlighted that PDE4 inhibitors **3c** was able to reduce IL-8 production. Other structural modifications are currently under investigation to enhance the activity and modulate physico-chemical properties of this class of compounds.

Acknowledgements

Financial support from the French National Centre for Scientific Research (CNRS), the Regional Council of Champagne–Ardenne (France), the French Ministry of Higher Education and Research (MESR) and the European Regional Development Fund (FEDER) to the PIAnET CPER project is acknowledged. C.B. thanks the Regional Council of Champagne–Ardenne (France) for a Ph.D. fellowship. A.M. Ph.D. fellowship is co-funded by Reims-Metropole and the European Union (Europe invests in Champagne-Ardenne with the European Regional Development Fund). Thanks are given to the Maison de la simulation de Champagne-Ardenne (Reims, France) and the Centre Régional Informatique et d'Applications Numériques de Normandie (CRIANN, Rouen, France) for the provision of computational facilities. Thanks to ANR-11-EMMA-028-03-03 and “Fonds Agir pour les Maladies Chroniques” for research support to A.B.

References

- [1] For reviews on pyridazinone scaffold see: a) W. Akhtar, M. Shaquiquzzaman, M. Akhter, G. Verma, M. F. Khan, M. M. Alam, The therapeutic journey of pyridazinone, *Eur. J. Med. Chem.* 123 (2016) 256-281; b) C.G. Wermuth, Are pyridazines privileged structure ? *Med. Chem. Commun.* 2 (2011) 935-941; c) S. Dubey, P.A. Bhosle, Pyridazinone: an important element of pharmacophore possessing broad spectrum of activity, *Med. Chem. Res.* 24 (2015) 3579-3598.
- [2] M. Asif, A mini review on biological activities of pyridazinone derivatives as antiulcer, antisecretory, antihistamine and particularly against histamine H₃R, *Mini Rev. Med. Chem.* 14 (2014) 1093-1103.
- [3] S. Demirayak, A.C. Karaburun, R. Beis, Some pyrrole substituted aryl pyridazinone and phthalazinone derivatives and their antihypertensive activities, *Eur. J. Med. Chem.* 39 (2004) 1089-1095.
- [4] W. Malinka, A. Redzicka, O. Lozach, New derivatives of pyrrolo[3,4-*d*]pyridazinone and their anticancer effects, *Il Farmaco* 59 (2004) 457-462.
- [5] I. G. Rathish, K. Javed, S. Ahmad, S. Bano, M. S. Alam, M. Akhter, K.K. Pillai, S. Ovais, M. Samim, Synthesis and evaluation of anticancer activity of some novel 6-aryl-2-(*p*-sulfamylphenyl)-pyridazin-3(2*H*)-ones, *Eur. J. Med. Chem.* 49 (2012) 304-309.
- [6] J. Singh, D. Sharma, R. Bansal, Pyridazinone: An attractive lead for anti-inflammatory and analgesic drug discovery, *Future Med. Chem.* 9 (2017) 95-127.
- [7] M. P. Giovannoni, C. Vergelli, C. Biancalani, N. Cesari, A. Graziano, P. Biagini, J. Gracia, A. Gavalda, V. Dal Paz, Novel pyrazolopyrimidopyridazinones with potent and selective phosphodiesterase 5 inhibitory activity as potential agents for treatment of erectile dysfunction, *J. Med. Chem.* 49 (2006) 5363-5371.
- [8] H. Amschler, Fluoroalkoxy-substituted benzamides and their use as cyclic nucleotide phosphodiesterase inhibitors, US Patent 5,712,298, 1998.
- [9] For reviews on PDE4 inhibitors in airways disease see: a) M. Houslay, P. Schafer, K. Zhang, Phosphodiesterase-4 as a therapeutic target, *Drug Discov. Today* 10 (2005) 1503-

1519; b) A. Kodimuthali, S.S.L. Jabaris, M. Pal, Recent advances on phosphodiesterase 4 inhibitors for the treatment of asthma and chronic obstructive pulmonary disease, *J. Med. Chem.* 71 (2008) 5471-5489; c) P.M.A. Calverley, Roflumilast in symptomatic chronic obstructive pulmonary disease: two randomised clinical trials, *Lancet.* 374 (2009) 685-694; d) M. DeNinno, Future directions in phosphodiesterase drug discovery, *Bioorg. Med. Chem. Lett.* 22 (2012) 6794-6800; e) A. Gavaldà, R.S. Roberts, Phosphodiesterase-4 inhibitors: a review of current developments (2010 - 2012), *Expert Opin. Ther. Pat.* 23 (2013) 997-1016; f) A. Martinez, C. Gil, cAMP-specific phosphodiesterase inhibitors: promising drugs for inflammatory and neurological diseases, *Expert Opin. Ther. Pat.* 24 (2014) 1311-1321; g) A.M. Mulhall, C.A. Droege, N.E. Ernst, R.J. Panos, M.A. Zafar, Phosphodiesterase 4 inhibitors for the treatment of chronic obstructive pulmonary disease: a review of current and developing drugs, *Expert Opin. Invest. Drugs* 24 (2015) 1597-1611.

[10] J. M. Michalski, G. Golden, J. Ikari, S.I. Rennard. PDE4: a novel target in the treatment of chronic obstructive pulmonary disease, *Clin. Pharmacol. Ther.* 91 (2012) 134-142.

[11] N. J. Press, K. H. Banner, PDE4 inhibitors - a review of the current field, *Prog. Med. Chem.* 47 (2009) 37-74.

[12] a) M. Cazzola, L. Calzetta, P. Rogliani, M.G. Matera, The discovery of Roflumilast for the treatment of COPD, *Expert Opin. Drug discovery* 11 (2016) 733-744; b) D.P. Tashkin, Roflumilast: the new orally active, selective PDE4 inhibitor for the treatment of COPD, *Expert Opin. Pharmacother.* 15 (2014) 85-96.

[13] H. Abdulrahim, S. Thistleton, A.O. Adebajo, T. Shaw, C. Edwards, A. Wells, Apremilast: a PDE4 inhibitor for the treatment of psoriasis arthritis, *Expert Opin. Pharmacother.* 16 (2015) 1099-1108.

[14] A. Kümmerle, M. Schmitt, S. V. S. Cardozo; C. Lugnier, P. Villa, A. B. Lopes, N. Romeiro, H. Justiniano, M. A. Martins, C. Fraga, J.-J. Bourguignon, A. Barreiro, Design, synthesis and pharmacological evaluation of *N*-acylhydrazones and novel conformationally constrained compounds as selective and potent orally active phosphodiesterase-4 inhibitors, *J. Med. Chem.* 55 (2012) 7525-7545.

[15] J. Gracia, M. A. Buil, J. Castro, P. Eichhorn, M. Ferrer, A. Gavaldà, B. Hernandez, V. Segarra, M.D. Lehner, I. Moreno, L. Pages, R. S. Roberts, J. Serrat, S. Sevilla, J. Taltavull, M. Andres, J. Cabedo, D. Vilella, E. Calama, C. Carcasona, M. Miralpeix, Biphenyl pyridazinone

derivatives as inhaled PDE4 inhibitors: structural biology and structure–activity relationships, *J. Med. Chem.* 59 (2016) 10479-10497.

[16] a) A. Sukhorukov, Y. Boyko, Y. Nelyubina, S. Gerard, S. Ioffe, V. Tartakovsky, L. Malleret, A. Belaaouaj, Synthesis of PDE IVb Inhibitors. 3. Synthesis of (+)-, (-)-, and (±)-7-[3-(cyclopentyloxy)-4-methoxyphenyl]hexahydro-3H-pyrrolizin-3-one via reductive domino transformations of 3-β-carbomethoxyethyl-substituted six-membered cyclic nitronates, *J. Org. Chem.* 77 (2012) 5465-5469; b) S. Gérard, J.-P. Bouillon, E. Hénon, A. Belaaouaj, Preparation of fluorinated pyridazin-3-ones as selective PDE4 inhibitors for treating lung diseases, WO patent 2016066973A1.

[17] Z.-Z. Zhou, B.-C. Ge, Q.-P. Zhong, C. Huang, Y.-F. Cheng, X.-M. Yang, H. Wang, J.-P. Xu, Development of highly potent phosphodiesterase 4 inhibitors with anti-neuroinflammation potential: Design, synthesis, and structure-activity relationship study of catecholamides bearing aromatic rings, *Eur. J. Med. Chem.* 124 (2016) 372-379.

[18] Q. Huai, H. Wang, Y. Sun, H.-Y. Kim, Y. Liu, H. Ke, Three-dimensional structures of PDE4D in complex with roliprams and implication on inhibitor selectivity, *Structure* 11 (2003) 865-873.

[19] S. Pieretti, L. Dominici, A. Di Giannuario, N. Cesari, V. Dal Piaz, Local anti-inflammatory effect and behavioral studies on new PDE4 inhibitors, *Life Sci.* 79 (2006) 791-800.

[20] V. Dal Piaz, M. P. Giovannoni, C. Castellana, J. M. Palacios, J. Beleta, T. Doménech, V. Segarra, Heterocyclic-fused 3(2H)-pyridazinones as potent and selective PDE IV inhibitors: further structure-activity relationships and molecular modelling studies, *Eur. J. Med. Chem.* 33 (1998) 789-797.

[21] M. Van der Mey, A. Hatzelmann, I. J. Van der Laan, G. J. Sterk, U. Thibaut, H. Timmerman, Novel Selective PDE4 Inhibitors. 1. Synthesis, Structure–Activity Relationships, and Molecular Modeling of 4-(3,4-Dimethoxyphenyl)-2H-phthalazin-1-ones and Analogues, *J. Med. Chem.* 44 (2001) 2511-2522.

[22] N. Chopin, H. Yanai, S. Iikawa, G. Pilet, J.-P. Bouillon, M. Médebielle, A rapid entry to diverse γ-ylidenetetronate derivatives through regioselective bromination of tetronic acid

derived γ -lactones and metal-catalyzed postfunctionalization, *Eur. J. Org. Chem.* 28 (2015) 6259-6269.

[23] For review on the chemistry of levulinic acid, see: B.V. Timokhin, V.A. Baransky, G.D. Eliseeva, Levulinic acid in organic synthesis, *Russ. Chem. Rev.* 68 (1999) 73-84 and references cited therein.

[24] M. Raoul, S. Gérard, J. Sapi, New Approach to the synthesis of *N*-alkylated-2-substituted azetidin-3-ones, *Eur. J. Org. Chem.* (2006) 2440-2445.

[25] S. Adachi, F. Tanaka, K. Watanabe, T. Harada, Oxazaborolidinone-catalyzed enantioselective Friedel–Crafts alkylation of furans and indoles with α,β -Unsaturated ketones, *Org. Lett.*, 11 (2009) 5206-5209.

[26] C. Barberot, J.-C. Boisson, S. Gérard, H. Khartabil, E. Thiriot, G. Monard, E. Hénon, AlgoGen: a tool coupling a linear scaling-quantum method with a genetic algorithm for exploring non-covalent interactions, *Comp. Theor. Chem.* 1028 (2014) 7-18.

[27] M. E. Lee, J. Markowitz, J.-O. Lee, H. Lee, Crystal structure of phosphodiesterase 4D and inhibitor complex1, *FEBS Lett.* 530 (2002) 53-58.

[28] C. Lefebvre, G. Rubez, H. Khartabil, J.-C. Boisson, J. Contreras-García, E. Hénon, Accurately extracting the signature of intermolecular interactions present in the NCI plot of the reduced density gradient *versus* electron density, *Phys. Chem. Chem. Phys.* 19 (2017) 17928-17936.

[29] A. Buenestado, S. Grassin-Delyle, F. Guitard, E. Naline, C. Faisy, D. Israël-Biet, E. Sage, JF. Bellamy, H. Tenor, P. Devillier, Roflumilast inhibits the release of chemokines and TNF- α from human lung macrophages stimulated with lipopolysaccharide, *Br. J. Pharmacol.* 165 (2012) 1877-1890.

[30] S. Kubo, M. Kobayashi, M. Iwata, K. Miyata, K. Takahashi, Y. Shimizu, Anti-neutrophilic inflammatory activity of ASP3258, a novel phosphodiesterase type 4 inhibitor, *Int. Immunopharmacol.* 12 (2012) 59-63.

[31] N.A. Jones, V. Boswell-Smith, R. Lever, CP. Page, The effect of selective phosphodiesterase isoenzyme inhibition on neutrophil function *in vitro*, *Pulm. Pharmacol. Ther.* 18 (2005) 93-101.

ACCEPTED MANUSCRIPT

Experimental section

Chemistry

General

Solvents : Solvents were dried and purified by standard literature methods prior to use.

Reagents : Reagents were bought from Acros Organics and Sigma-Aldrich and were used without further purification.

Instrumentation : Reactions were monitored on silicagel plates (Silicagel 60F254 from Merck) and column chromatography was carried out on silica gel 60 (70-200 μm).

Proton and Carbon Nuclear Magnetic Resonance spectra (^1H NMR ^{13}C NMR) were recorded on a Bruker DPX 300 apparatus at 300 and 75 MHz respectively, in CDCl_3 . Chemical shifts are reported in parts per million (ppm) downfield from tetramethylsilane (TMS) as internal standard followed by multiplicity in which s, bs, d, t, q, dd, dt, td, tt, m are respectively singlet, broad singlet, doublet, triplet, quadruplet, dedoubled doublet, dedoubled triplet, detripled doublet, detripled triplet and multiplet (or unwell-resolved signals). Coupling constants J are quoted in Hertz (Hz). Bidimensional NMRs (COSY, HSQC and HMBC) were used to assign signals.

Infrared spectra (IR) (thin film or KBr pastille) were measured on a Perkin-Elmer SPECTRUM BX/RX Fourier transform spectrometer. Principal absorption bands are given in cm^{-1} .

Electronic Impact (EI), Chemical Ionisation (CI), ElectroSpray Ionisation (ESI) Mass Spectra (MS) and High Resolution Mass Spectra (HRMS) were either recorded with an ESI-Q-TOF mass spectrometer from Waters or with a GCT CA 170 Micromass Waters apparatus. The (+)ESI Mass Spectra were performed in a positive mode with CH_3OH as solvent. The masses are measured in Dalton (Da). 5-Arylidene-tetronate precursors were prepared by *in situ* aldolisation/dehydration sequence according to reference 18.

General procedure for the formation of the 5-alkoxy-pyridazinone **1a-f**:

To a solution of furan-2(5H)-one (1 eq.) in methanol (10 mL/1 mmol) is added hydrazine (from 2 to 5 eq.). The mixture is stirred at reflux during 12 hours. After cooling, the pyridazinone usually precipitates. The solid is then filtered and washed with a little amount of cold methanol to afford the desired compound. The mother liquor is then evaporated under reduced pressure and the resulting residue is recrystallized in hot MeOH or diethyl ether (for compounds **1a,c,e**) or is chromatographed on silica gel (eluent: petroleum ether/AcOEt or $\text{CH}_2\text{Cl}_2/\text{AcOEt}$, for compounds **1b,d,f**). Overall yields were calculated on the combined fractions.

5-Methoxy-6-benzylpyridazin-3(2H)-one 1a. According to the general procedure, and starting from 100 mg of (Z)-4-methoxy-5-benzylidene-furan-2(5H)-one and 80 μL of hydrazine (35 % w/t in water), pure compound **1a** is obtained after filtration followed by recrystallisation in methanol as a white powder. Yield: 55 mg (52 %).

Mp: 125-127 °C. $^1\text{H NMR}$ (300 MHz, CD_3OD) δ (ppm) = 3.84 (s, 3 H), 3.95 (s, 2 H), 6.22 (s, 1 H), 7.1-7.3 (m, 5 H). $^{13}\text{C NMR}$ (75 MHz, CD_3OD) δ (ppm) = 35.5, 56.0, 103.2, 126.3, 128.3 (2 C), 128.7 (2 C), 137.6, 141.6, 159.6, 162.6. **IR** (KBr) ν (cm^{-1}) = 3200, 2943, 2866, 1677, 1625, 1589, 1451, 1245. **MS** (ESI⁺) m/z 455 [2M+Na]⁺, 433 [2M+H]⁺, 239 [M+Na]⁺, 217 [M+H]⁺.

5-Methoxy-6-benzyl-2-methylpyridazin-3(2H)-one 1b. According to the general procedure, and starting from 110 mg of (Z)-4-methoxy-5-benzylidene-furan-2(5H)-one and 153 μL of methylhydrazine, pure compound **1b** is obtained after chromatography on silica gel (eluent: petroleum ether/AcOEt, 2/8) as a white powder. Yield: 51 mg (41 %).

Mp: 239-241 °C. $^1\text{H NMR}$ (300 MHz, CD_3OD) δ (ppm) = 3.71 (s, 3 H), 3.84 (s, 3 H), 3.96 (s, 2 H), 6.26 (s, 1 H), 7.2-7.4 (m, 5 H). **IR** (KBr) ν (cm^{-1}) = 3027, 2942, 1650, 1591, 1455, 1404, 1336, 1243, 1225. **HRMS** (ESI; [M+Na]⁺) calculated for $\text{C}_{13}\text{H}_{14}\text{N}_2\text{O}_2\text{Na}$ 253.0953, found 253.0950.

5-Benzyloxy-6-benzylpyridazin-3(2H)-one 1c. According to the general procedure, and starting from 60 mg of (Z)-4-benzyloxy-5-benzylidene-furan-2(5H)-one and 34 μL of hydrazine (35 % w/t in water), pure compound **1c** is obtained after filtration followed by recrystallisation in methanol as a white powder. Yield: 17 mg (27 %).

Mp: 221-223 °C. $^1\text{H NMR}$ (300 MHz, DMSO-d_6) δ (ppm) = 3.88 (s, 2 H), 5.10 (s, 2 H), 6.25 (s, 1 H), 7.1-7.5 (m, 10 H), 12.5 (bs, 1 H). $^{13}\text{C NMR}$ (75 MHz, DMSO-d_6) δ (ppm) = 35.9, 69.7, 104.3, 126.3, 127.6 (2C), 128.2, 128.3 (2C), 128.4 (2C), 128.7 (2C), 135.2, 137.6, 141.7, 158.4, 162.6. **IR** (KBr) ν (cm^{-1}) = 3200, 3061, 2966, 2854, 1753, 1627, 1590, 1555, 1451, 1422, 1256. **HRMS** (ESI; [M+H]⁺) calculated for $\text{C}_{18}\text{H}_{17}\text{N}_2\text{O}_2$ 293.1290, found 293.1284.

5-Benzyloxy-6-benzyl-2-methylpyridazin-3(2H)-one 1d. According to the general procedure, and starting from 150 mg of (Z)-4-benzyloxy-5-benzylidene-furan-2(5H)-one and 152 μL of methylhydrazine, pure compound **1d** is obtained after chromatography on silica gel (eluent: petroleum ether/AcOEt, 2/8) as a white powder. Yield: 83 mg (50 %).

Mp: 161-163 °C. $^1\text{H NMR}$ (300 MHz, CD_3OD) δ (ppm) = 3.73 (s, 3 H), 3.98 (s, 2 H), 5.08 (s, 2 H), 6.31 (s, 1 H), 7.1-7.5 (m, 10 H). $^{13}\text{C NMR}$ (75 MHz, DMSO-d_6) δ (ppm) = 36.0, 38.6, 69.9, 104.1,

126.4, 127.5 (2C), 128.1, 128.3 (2C), 128.4 (2C), 128.5 (2C), 135.1, 137.5, 141.3, 157.9, 161.1. **IR** (KBr) ν (cm⁻¹) = 3025, 2933, 1657, 1593, 1436, 1375, 1338, 1245. **HRMS** (ESI; [M+H]⁺) calculated for C₁₉H₁₉N₂O₂ 307.1447, found 307.1450.

5-(Benzyloxy)-6-(3,4-dimethoxybenzyl)pyridazin-3(2H)-one *1e*. According to the general procedure, and starting from 33 mg of (Z)-4-benzyloxy-5-(3,4-dimethoxybenzylidene)furan-2(5H)-one and 18 μ L of hydrazine (35 % w/t in water), pure compound ***1e*** is obtained after filtration followed by recrystallisation in diethyl ether as a beige powder. Yield: 30 mg (88 %).

Mp: 166-168 °C. **¹H NMR** (300 MHz, CDCl₃) δ (ppm) = 3.69 (s, 3 H), 3.86 (s, 3 H), 3.88 (s, 2 H), 4.97 (s, 2 H), 6.17 (s, 1 H), 6.68-6.78 (m, 3 H), 7.21-7.24 (m, 2 H), 7.36-7.38 (m, 3 H), 10.47 (bs, 1 H). **¹³C NMR** (75 MHz, CDCl₃) δ (ppm) = 36.5, 55.8, 56.0, 70.7, 104.3, 111.2, 112.4, 121.1, 127.9 (2 C), 128.8 (3 C), 129.7, 134.3, 143.8, 147.8, 148.8, 159.7, 164.5. **MS** (EI) m/z 352 [M⁺], 261, 230, 227, 91. **HRMS** (EI; [M⁺]) calculated for C₂₀H₂₀N₂O₄ 352.1423, found 352.1429.

5-(Benzyloxy)-6-(3,4-dimethoxybenzyl)-2-methylpyridazin-3(2H)-one *1f*. According to the general procedure, and starting from 15 mg of (Z)-4-benzyloxy-5-(3,4-dimethoxybenzylidene)furan-2(5H)-one and 14 μ L of methylhydrazine, pure compound ***1f*** is obtained after flash column chromatography (dichloromethane/ethyl acetate, from 8/2 to 7/3) as a yellow solid. Yield: 10 mg (59 %).

Mp: 140-142 °C. **¹H NMR** (300 MHz, CDCl₃) δ (ppm) = 3.68 (s, 3 H), 3.74 (s, 3 H), 3.85 (s, 3 H), 3.89 (s, 2 H), 4.95 (s, 2 H), 6.22 (s, 1 H), 6.69-6.78 (m, 3 H), 7.18-7.21 (m, 2 H), 7.34-7.36 (m, 3 H). **¹³C NMR** (75 MHz, CDCl₃) δ (ppm) = 36.6, 39.5, 55.8, 56.0, 70.7, 104.4, 111.2, 112.4, 121.0, 127.8 (2 C), 128.8, 128.9 (2 C), 130.0, 134.5, 142.6, 147.8, 148.9, 158.7, 162.5. **MS** (EI) m/z 366 [M⁺], 275, 244, 227, 105, 91. **HRMS** (EI; [M⁺]) calculated for C₂₁H₂₂N₂O₄ 366.1580, found 366.1586.

Typical procedure for the formation of ethyl 4-oxopent-2-enoate:

Ethyl 4-oxopent-2-enoate. Levulinic acid (1 eq) is dissolved in ethanol. Catalytic amount of sulfuric acid (0.1 eq) is added to the solution. The mixture is then stirred and headed at reflux. After 16 h, the reaction is stopped and the solvent is evaporated under reduced pressure to yield the ethyl levulinate in quantitative yield. Then bromine (1 eq) is dropwise added (during a period of 1 hour) to a cold (0°C) solution of ethyl levulinate (1 eq) in chloroform. After 30 minutes of stirring at 0°C, triethylamine (3 eq) is then dropwise added during 1 hour. The mixture is stirred for 1h30 after which water is added to the solution. The crude mixture is then extracted by dichloromethane and the combined organic phases are washed successively with aqueous solutions of hydrochloric acid (10 %) and saturated ammonium chloride, dried over anhydrous MgSO₄ and concentrated under reduced pressure. The crude mixture is

purified by flash chromatography over silica gel using dichloromethane as eluent to yield 47 % of a yellow oil. **¹H NMR** (300 MHz, CDCl₃) δ (ppm) = 1.33 (t, *J*= 7.1 Hz, 3 H), 2.37 (s, 3 H), 4.28 (q, *J*= 7.1 Hz, 2 H), 6.65 (d, *J*= 16.1 Hz, 1 H), 7.02 (d, *J*= 16.1 Hz, 1 H). **¹³C NMR** (75 MHz, CDCl₃) δ (ppm) = 14.2, 27.6, 60.4, 135.3, 139.7, 165.7, 196.8. **IR** (KBr) ν (cm⁻¹) = 3052, 2982, 1721, 1701, 1422, 1291, 1263, 1157. **MS** (CI) *m/z* 143 [M+H]⁺, 129. **HRMS** (CI; [M+H]⁺) calculated for C₇H₁₁O₃ 143.0751, found 143.0708.

General procedure for Friedel-Crafts alkylation:

Ethyl 4-oxopenten-2-oate (1 eq) is dissolved in toluene. One equivalent of heterocyclic compound is added to the solution with a catalytic amount of *para*-toluenesulfonic acid (PTSA, 0.1 eq). The reaction is stirred and heated at reflux. After about 48 hours (monitoring by thin layer chromatography), the reaction is stopped and the solvent is evaporated under reduced pressure. The crude mixture is then purified by column chromatography and sometimes crystallized in diethyl ether.

Ethyl 2-(1*H*-indol-3-yl)-4-oxo-pentanoate 2a. According to the general procedure for Friedel-Crafts alkylation, starting from 147 mg of ethyl 4-oxopenten-2-oate and 120 mg of indole, the title compound is isolated after column chromatography (cyclohexane/AcOEt=7/3) followed by recrystallization in diethyl ether as a beige powder. Yield: 139 mg (53 %).

Mp: 116-118 °C. **¹H NMR** (300 MHz, CDCl₃) δ (ppm) = 1.18 (t, *J*= 7.1 Hz, 3 H), 2.17 (s, 3 H), 2.83 (dd, *J*= 17.9, 4.4 Hz, 1 H), 3.51 (dd, *J*= 18.0, 10.2 Hz, 1 H), 4.01-4.22 (m, 2 H), 4.39 (dd, *J*= 10.2, 4.5 Hz, 1 H), 7.05 (d, *J*= 2.7 Hz, 1 H), 7.10-7.22 (m, 2 H), 7.34 (d, *J*= 8.1 Hz, 1 H), 7.71 (d, *J*= 7.8 Hz, 1 H), 8.25 (bs, 1 H). **¹³C NMR** (75 MHz, CDCl₃) δ (ppm) = 14.2, 30.1, 38.0, 46.3, 61.2, 111.5, 113.0, 119.3, 119.8, 122.2, 122.4, 126.2, 136.4, 173.9, 207.1. **IR** (KBr) ν (cm⁻¹) = 3405, 2919, 1721, 1708, 1457, 1413, 1361, 1336, 1323, 1258, 1232, 1173, 1090. **MS** (EI) *m/z* 259 [M⁺], 213, 186, 144, 115. **HRMS** (EI; [M⁺]) calculated for C₁₅H₁₇NO₃ 259.1208, found 259.1212.

Ethyl 2-(1*H*-methyl-indol-3-yl)-4-oxo-pentanoate 2b. According to the general procedure for Friedel-Crafts alkylation with 157 mg of ethyl 4-oxopenten-2-oate and 133 mg of 1-methylindole, the mixture is heated at reflux during 65 h. The title compound is isolated after column chromatography (cyclohexane/ ethyl acetate =8/2) as a brown lacquer. Yield: 153 mg (56 %).

¹H NMR (300 MHz, CDCl₃) δ (ppm) = 1.20 (t, *J*= 7.1 Hz, 3 H), 2.18 (s, 3 H), 2.83 (dd, *J*= 18.0, 4.5 Hz, 1 H), 3.49 (dd, *J*= 18.0, 10.2 Hz, 1 H), 3.74 (s, 3 H), 4.02 (q, *J*= 7.1 Hz, 2 H), 4.37 (dd, *J*= 10.2, 4.5 Hz, 1 H), 6.96 (s, 1 H), 7.10-7.31 (m, 3 H), 7.69 (d, *J*= 7.9 Hz, 1 H). **¹³C NMR** (75 MHz, CDCl₃) δ (ppm) = 14.2, 30.1, 32.9, 37.8, 46.6, 61.1, 109.5, 111.4, 119.4, 119.5, 122.0, 126.6, 126.8, 137.1,

173.9, 207.0. **IR** (KBr) ν (cm^{-1}) = 3426, 2925, 1721, 1609, 1542, 1470, 1369, 1328, 1155, 1015. **MS** (EI) m/z 273 [M^+], 227, 225, 216, 200, 158, 156. **HRMS** (EI; [M^+]) calculated for $\text{C}_{16}\text{H}_{19}\text{NO}_3$ 273.1365, found 273.1368.

Ethyl 2-(5-methoxy-1H-indol-3-yl)-4-oxo-pentanoate 2c. According to the general procedure for Friedel-Crafts alkylation using 154 mg of ethyl 4-oxopenten-2-oate and 151 mg of 5-methoxyindole, the title compound is isolated after column chromatography (cyclohexane/ ethyl acetate =7/3) as beige crystals. Yield: 198 mg (55 %).

Mp: 137-139 °C. **$^1\text{H NMR}$** (300 MHz, CDCl_3) δ (ppm) = 1.21 (t, J = 7.2 Hz, 3 H), 2.20 (s, 3 H), 2.83 (dd, J = 18.0, 4.4 Hz, 1 H), 3.50 (dd, J = 18.0, 10.4 Hz, 1 H), 3.87 (s, 3 H), 4.02-4.24 (m, 2 H), 4.35 (dd, J = 10.4, 4.4 Hz, 1 H), 6.87 (dd, J = 9.0, 2.4 Hz, 1 H), 7.06 (d, J = 2.4 Hz, 1 H), 7.16 (d, J = 2.4 Hz, 1 H), 7.24 (d, J = 8.7 Hz, 1 H), 8.01 (bs, 1 H). **$^{13}\text{C NMR}$** (75 MHz, CDCl_3) δ (ppm) = 14.2, 30.1, 37.9, 46.1, 56.0, 61.1, 100.9, 112.2, 112.5, 112.8, 122.8, 126.6, 131.4, 154.2, 173.9, 207.2. **IR** (KBr) ν (cm^{-1}) = 3333, 2925, 1718, 1708, 1620, 1581, 1483, 1457, 1364, 1302, 1266, 1199, 1170, 1023. **MS** (EI) m/z 289 [M^+], 243, 216, 174, 159, 130, 115. **HRMS** (EI; [M^+]) calculated for $\text{C}_{16}\text{H}_{19}\text{NO}_4$ 289.1314, found 289.1309.

Ethyl 2-(3-methyl-1H-indol-2-yl)-4-oxo-pentanoate 2d. According to the general procedure for Friedel-Crafts alkylation starting from 142 mg of ethyl 4-oxopenten-2-oate and 136 mg of 3-methylindole, the title compound is isolated after column chromatography (cyclohexane/ ethyl acetate =6/4) as a brown solid. Yield: 188 mg (69 %).

Mp: 115-117 °C. **$^1\text{H NMR}$** (300 MHz, CDCl_3) δ (ppm) = 1.15 (t, J = 7.2 Hz, 3 H), 2.16 (s, 3 H), 2.45 (s, 3 H), 2.75 (dd, J = 18.0, 5.0 Hz, 1 H), 3.63 (dd, J = 18.0, 9.3 Hz, 1 H), 3.97-4.21 (m, 2 H), 4.37 (dd, J = 9.3, 5.0 Hz, 1 H), 7.04-7.14 (m, 2 H), 7.25-7.28 (m, 2 H), 7.59 (dd, J = 7.8, 1.5 Hz, 1 H), 7.83 (bs, 1 H). **$^{13}\text{C NMR}$** (75 MHz, CDCl_3) δ (ppm) = 12.1, 14.3, 30.4, 37.4, 45.3, 61.1, 108.5, 110.5, 118.8, 119.7, 121.3, 127.2, 132.4, 135.3, 173.8, 207.2. **IR** (KBr) ν (cm^{-1}) = 2971, 2919, 1721, 1702, 1454, 1392, 1369, 1346, 1320, 1248, 1214, 1160, 1088. **MS** (EI) m/z 273 [M^+], 227, 216, 200, 158, 130. **HRMS** (EI; [M^+]) calculated for $\text{C}_{16}\text{H}_{19}\text{NO}_3$ 273.1365, found 273.1367.

Ethyl 2-(benzotriazol-1-yl)-4-oxo-pentanoate 2e. According to the general procedure for Friedel-Crafts alkylation starting from 148 mg of ethyl 4-oxopenten-2-oate and 125 mg of 1,2,3-benzotriazole, the title compound is isolated after column chromatography (cyclohexane/ ethyl acetate =7/3) as a brown oil. Yield: 164 mg (65 %).

¹H NMR (300 MHz, CDCl₃) δ (ppm) = 1.15 (t, *J* = 7.1 Hz, 3 H), 2.26 (s, 3 H), 3.65 (dd, *J* = 18.2, 7.4 Hz, 1 H), 3.79 (dd, *J* = 18.0, 6.0 Hz, 1 H), 4.12-4.23 (m, 2 H), 5.98 (dd, *J* = 7.4, 6.2 Hz, 1 H), 7.37-7.42 (m, 1 H), 7.50-7.56 (m, 1 H), 7.63 (d, *J* = 8.4 Hz, 1 H), 8.07 (d, *J* = 8.4 Hz, 1 H). **¹³C NMR** (75 MHz, CDCl₃) δ (ppm) = 14.0, 30.1, 44.1, 56.1, 62.7, 109.7, 120.1, 124.4, 128.0, 133.4, 145.8, 168.0, 204.0. **IR** (KBr) ν (cm⁻¹) = 3054, 2982, 2925, 1746, 1718, 1615, 1591, 1491, 1449, 1405, 1367, 1269, 1204, 1163, 1104, 1015. **MS** (EI) *m/z* 261 [M⁺], 204, 188, 160, 127, 118, 97, 91. **HRMS** (EI; [M⁺]) calculated for C₁₃H₁₅N₃O₃ 261.1113, found 261.1115.

Ethyl 2-morpholinyl-4-oxopentanoate 2f. According to the general procedure for Friedel-Crafts alkylation starting from 284 mg of ethyl 4-oxopenten-2-oate and 174 mg of morpholine, the title compound is isolated after column chromatography (dichloromethane/methanol=9.5/0.5) as a yellow oil. Yield: 348 mg (76 %).

¹H NMR (300 MHz, CDCl₃) δ (ppm) = 1.22 (t, *J* = 7.1 Hz, 3 H), 2.12 (s, 3 H), 2.47-2.54 (m, 2 H), 2.64-2.75 (m, 3 H), 2.97 (dd, *J* = 17.1, 9.2 Hz, 1 H), 3.65-3.75 (m, 5 H), 4.16-4.25 (m, 2 H). **¹³C NMR** (75 MHz, CDCl₃) δ (ppm) = 14.4, 30.2, 42.9, 50.2 (2 C), 60.7, 63.0, 67.3 (2 C), 170.6, 206.2. **IR** (KBr) ν (cm⁻¹) = 3602, 3411, 2961, 2853, 1724, 1713, 1362, 1166, 1111. **MS** (EI) *m/z* 229 [M⁺], 184, 156, 127, 114. **HRMS** (EI; [M⁺]) calculated for C₁₁H₁₉NO₄ 229.1314, found 229.1317.

Diethyl 2,2'-(piperazine-1,4-diyl)bis(4-oxopentanoate) 2g. According to the general procedure for Friedel-Crafts alkylation with 284 mg of ethyl 4-oxopenten-2-oate and 172 mg of piperazine, the compound (yellow oil) isolated after column chromatography (dichloromethane/methanol=9.5/0.5) is the corresponding dimere adduct (Yield: 38%).

¹H NMR (300 MHz, CDCl₃) δ (ppm) = 1.33 (t, *J* = 7.1 Hz, 6 H), 2.18 (s, 6 H), 2.48 (t, *J* = 7.8 Hz, 2 H), 2.63-2.73 (m, 10 H), 3.08 (dd, *J* = 17.1, 9.3 Hz, 2 H), 3.73 (dd, *J* = 9.2, 5.0 Hz, 2 H), 4.18 (q, *J* = 7.1 Hz, 4 H). **MS** (EI) *m/z* 370 [M⁺], 327, 297, 239, 155, 127, 97. **HRMS** (EI; [M⁺]) calculated for C₁₈H₃₀N₂O₆ 370.2104, found 370.2111.

Ethyl 4-oxo-2-(4-methylpiperazin-1-yl)-pentanoate 2h. According to the general procedure for Friedel-Crafts alkylation starting from 207 mg of ethyl 4-oxopenten-2-oate and 160 μL of 1-methylpiperazine, the compound is obtained after column chromatography (dichloromethane/methanol=9/1) as a yellow oil. Yield: 202 mg (57 %).

¹H NMR (300 MHz, CDCl₃) δ (ppm) = 1.22 (t, *J* = 7.1 Hz, 3 H), 2.11 (s, 3 H), 2.23 (s, 3 H), 2.32-2.51 (m, 6 H), 2.60 (dd, *J* = 17.0, 5.3 Hz, 1 H), 2.66-2.73 (m, 2 H), 2.99 (dd, *J* = 17.1, 9.3 Hz, 1 H), 3.69 (dd, *J* = 9.3, 5.1 Hz, 1 H), 4.11 (q, *J* = 7.2 Hz, 2 H). **¹³C NMR** (75 MHz, CDCl₃) δ (ppm) = 14.4, 29.7,

30.3, 43.0 (2 C), 45.7, 48.2, 55.3 (2 C), 60.7, 62.7, 170.7, 206.4. **MS** (EI) m/z 242 [M^+], 199, 169, 127, 100. **HRMS** (EI; [M^+]) calculated for $C_{12}H_{22}N_2O_3$ 242.1630, found 242.1633.

General procedure for the formation of the 4,5-dihydropyridazin-3(2H)-one **3a-h**:

Method a) Hydrazine (1.5 eq) is added to a solution of precursor (1 eq) in ethanol (0.2 M). The mixture is stirred at room temperature and the reaction is monitored by TLC. After total conversion, evaporation under reduced pressure provided the corresponding 4,5-dihydropyridazinone which could be purified by silica gel column chromatography.

Method b) Hydrazine (12.5 eq) is added to a solution of precursor (1 eq) in acetic acid (0.15 M). The mixture is stirred at reflux and the reaction is monitored by TLC. After total conversion, evaporation under reduced pressure provided the corresponding 4,5-dihydropyridazinone which could be purified by silica gel column chromatography.

4-(1H-Indol-3-yl)-6-methyl-4,5-dihydropyridazin-3(2H)-one 3a. According to the general procedure for the formation of the dihydropyridazinone cycle (method a)) starting from 70 mg of ethyl 2-(3-1H-indole)-4-oxo-pentanoate **2a** and 24 μ L of hydrazine hydrate. The desired compound is obtained after flash column chromatography (dichloromethane/methanol=9.6/0.4) followed by a recrystallization in dichloromethane, as a brown powder. Yield: 42 mg (61 %).

Mp: 244-246 °C. $^1\text{H NMR}$ (300 MHz, DMSO-*d*6) δ (ppm) = 2.00 (s, 3 H), 2.71-2.87 (m, 2 H), 3.83 (dt, J = 7.4, 1.1 Hz, 1 H), 6.97 (dt, J = 7.1, 1.1 Hz, 1 H), 7.05-7.10 (m, 2 H), 7.34 (d, J = 8.1 Hz, 1 H), 7.61 (d, J = 7.8 Hz, 1 H), 10.51 (bs, 1 H), 10.95 (bs, 1 H). $^{13}\text{C NMR}$ (75 MHz, DMSO-*d*6) δ (ppm) = 22.8, 32.4, 33.8, 111.3, 111.4, 118.5, 119.3, 121.2, 122.3, 126.4, 136.3, 151.9, 167.4. **IR** (KBr) ν (cm^{-1}) = 3366, 2914, 1667, 1455, 1416, 1374, 1330, 1248, 1222, 1173, 1101, 1013. **MS** (EI) m/z 227 [M^+], 198, 157, 143, 129, 115. **HRMS** (EI; [M^+]) calculated for $C_{13}H_{13}N_3O$ 227.1059, found 227.1057.

6-Methyl-4-(1-methyl-1H-indol-3-yl)-4,5-dihydropyridazin-3(2H)-one 3b. According to the general procedure for the formation of the dihydropyridazinone cycle (method a)) starting from 55 mg of ethyl 2-(1H-methylindol-3-yl)-4-oxo-pentanoate **2b** and 18 μ L of hydrazine hydrate. The desired compound is obtained after flash column chromatography (dichloromethane/ethyl acetate=8/2 to 7/3) as a beige lacquer. Yield: 26 mg (53 %).

$^1\text{H NMR}$ (300 MHz, CD_3OD) δ (ppm) = 2.03 (s, 3 H), 2.87 (ddd, J = 21.3, 16.8, 7.2, Hz, 2 H), 3.75 (s, 3 H), 3.97 (dt, J = 7.2, 0.6 Hz, 1 H), 6.99 (s, 1 H), 7.05 (dt, J = 6.9, 0.9 Hz, 1 H), 7.18 (dt, J = 7.2, 1.1 Hz, 1 H), 7.34 (d, J = 8.1 Hz, 1 H), 7.61 (d, J = 8.1 Hz, 1 H). $^{13}\text{C NMR}$ (75 MHz, CDCl_3) δ (ppm) = 23.4, 32.9, 33.8, 34.4, 109.7, 110.2, 119.2, 119.6, 122.2, 126.4, 126.7, 137.3, 153.5, 168.3. **MS** (EI)

m/z 241 [M^+], 212, 171, 157, 143, 115. **HRMS** (EI; [M^+]) calculated for $C_{14}H_{15}N_3O$ 241.1215, found 241.1217.

4-(5-Methoxy-1H-indol-3-yl)-6-methyl-4,5-dihydropyridazin-3(2H)-one 3c. According to the general procedure for the formation of the dihydropyridazinone cycle (method a)) starting from 80 mg of ethyl 2-(5-methoxy-1H-indol-3-yl)-4-oxo-pentanoate **2c** and 22 μ L of hydrazine hydrate. The desired compound is obtained after flash column chromatography (dichloromethane/methanol=9.6/0.4) followed by a recrystallization in dichloromethane as a beige powder. Yield: 55 mg (76 %)

Mp: 225-227 °C. **1H NMR** (300 MHz, CD_3OD) δ (ppm) = 2.05 (s, 3 H), 2.81-2.97 (m, 2 H), 3.82 (s, 3 H), 3.96 (dt, J = 6.9, 0.6 Hz, 1 H), 6.77 (dd, J = 8.7, 2.4 Hz, 1 H), 7.02 (s, 1 H), 7.12 (d, J = 2.4 Hz, 1 H), 7.23 (dd, J = 8.7, 0.6 Hz, 1 H). **^{13}C NMR** (75 MHz, $DMSO-d_6$) δ (ppm) = 22.9, 32.3, 33.7, 55.3, 101.2, 111.0, 111.3, 112.0, 122.9, 126.8, 131.4, 152.0, 153.0, 167.4. **MS** (EI) m/z 257 [M^+], 187, 159. **HRMS** (EI; [M^+]) calculated for $C_{14}H_{15}N_3O_2$ 257.1164, found 257.1164.

6-Methyl-4-(3-methyl-1H-indol-2-yl)-4,5-dihydropyridazin-3(2H)-one 3d. According to the general procedure for the formation of the dihydropyridazinone cycle (method a)) starting from 80 mg of ethyl 2-(3-methyl-1H-indol-2-yl)-4-oxo-pentanoate **2d** and 23 μ L of hydrazine hydrate. The desired compound is obtained after flash column chromatography (dichloromethane/ethyl acetate=5/5) followed by a recrystallization in dichloromethane as a white powder. Yield: 38 mg (54 %).

Mp: 225-227 °C. **1H NMR** (300 MHz, CD_3OD) δ (ppm) = 2.04 (s, 3 H), 2.36 (s, 3 H), 2.71 (dd, J = 17.4, 7.8 Hz, 1 H), 2.89 (ddd, J = 17.1, 12.3, 0.9 Hz, 1 H), 4.01 (dd, J = 12.3, 7.5 Hz, 1 H), 6.93 (dt, J = 8.1, 1.5 Hz, 1 H), 7.00 (dt, J = 7.2, 1.5 Hz, 1 H), 7.24 (d, J = 7.8 Hz, 1 H), 7.34 (d, J = 7.8 Hz, 1 H). **^{13}C NMR** (75 MHz, $DMSO-d_6$) δ (ppm) = 11.5, 22.6, 33.0, 33.2, 107.5, 110.5, 118.0, 118.1, 119.9, 126.8, 132.8, 135.3, 152.5, 168.1. **MS** (EI) m/z 241 [M^+], 171, 143, 130, 115. **HRMS** (EI; [M^+]) calculated for $C_{14}H_{15}N_3O$ 241.1215, found 241.1214.

4-(1H-Benzotriazol-1-yl)-6-methyl-4,5-dihydropyridazin-3(2H)-one 3e. According to the general procedure for the formation of the dihydropyridazinone cycle (method a)) starting from 93 mg of ethyl 2-(benzotriazol-1-yl)-4-oxo-pentanoate **2e** and 50 μ L of hydrazine (35 % wt in water). The desired compound is obtained after column chromatography (dichloromethane/ethyl acetate = 7/3 to 5/5) as a yellow oil. Yield: 12 mg (15 %).

1H NMR (300 MHz, $DMSO-d_6$) δ (ppm) = 2.08 (s, 3 H), 3.14 (dd, J = 16.8, 7.2 Hz, 1 H), 3.50 (dd, J = 16.8, 13.2 Hz, 1 H), 6.05 (dd, J = 13.2, 7.2 Hz, 1 H), 7.43 (ddd, J = 8.4, 6.9, 0.9 Hz, 1 H), 7.57 (ddd, J = 8.4, 6.9, 0.9 Hz, 1 H), 7.85 (d, J = 8.4 Hz, 1 H), 8.08 (d, J = 8.4 Hz, 1 H), 11.05 (s, 1 H). **^{13}C NMR** (75

MHz, DMSO-*d*₆) δ (ppm) = 22.7, 31.2, 52.5, 111.1, 119.2, 124.2, 127.5, 133.6, 145.1, 152.5, 162.7. **MS** (EI) m/z 229 [M^+], 159, 119, 110. **HRMS** (EI; [M^+]) calculated for C₁₁H₁₁N₅O 229.0964, found 229.0968.

6-Methyl-4-morpholino-4,5-dihydropyridazin-3(2H)-one 3f. According to the general procedure for the formation of the dihydropyridazinone cycle (method a)) starting from 150 mg of ethyl 2-morpholino-4-oxopentanoate **2f** and 92 μ L of hydrazine (35 % wt in water). The desired compound is obtained as a yellow oil. Yield: 58 mg (45 %).

¹H NMR (300 MHz, CD₃OD) δ (ppm) = 2.04 (s, 3 H), 2.40-2.48 (m, 1 H), 2.60-2.72 (m, 4 H), 3.15-3.29 (m, 1 H), 3.66-3.71 (m, 5 H). **¹³C NMR** (75 MHz, CDCl₃) δ (ppm) = 22.9, 29.6, 49.5 (2 C), 58.3, 67.0 (2 C), 153.0, 165.3. **IR** (KBr) ν (cm⁻¹) = 3421, 2858, 1656, 1649, 1602, 1551, 1432, 1380, 1334, 1135, 1106. **MS** (EI) m/z 197 [M^+], 112, 111, 110, 87, 86, 82, 81, 57, 53. **HRMS** (EI; [M^+]) calculated for C₉H₁₅N₃O₂ 197.1164, found 197.1171.

2,6-Dimethyl-4-morpholino-4,5-dihydropyridazin-3(2H)-one 3g. According to the general procedure for the formation of the dihydropyridazinone cycle (method a)) starting from 150 mg of ethyl 2-morpholino-4-oxopentanoate **2f** and 53 μ L of methylhydrazine. The desired compound is obtained after flash column chromatography (dichloromethane/methanol = 9.8/0.2) as a yellow oil. Yield: 65 mg (48 %).

¹H NMR (300 MHz, CDCl₃) δ (ppm) = 2.08 (s, 3 H), 2.62-2.64 (m, 6 H), 3.22 (t, J = 7.2 Hz, 1 H), 3.33 (s, 3 H), 3.69-3.72 (m, 4 H). **¹³C NMR** (75 MHz, CDCl₃) δ (ppm) = 23.3, 30.4, 36.2, 50.0 (2 C), 59.0, 67.2 (2 C), 152.9, 163.5. **MS** (EI) m/z 211 [M^+], 124, 96, 87. **HRMS** (EI; [M^+]) calculated for C₁₀H₁₇N₃O₂ 211.1321, found 211.1321.

6-Methyl-4-(4-methylpiperazin-1-yl)-4,5-dihydropyridazin-3(2H)-one 3h. According to the general procedure for the formation of the dihydropyridazinone cycle (method a)) starting from 500 mg of ethyl 4-oxo-2-(4-methylpiperazin-1-yl)-pentanoate **2h** and 280 μ L of hydrazine (35 % wt in water). The desired compound is obtained after flash column chromatography (dichloromethane/methanol gradient=9.8/0.2 to 7/3) as a yellow lacquer. Yield: 369 mg (85 %).

¹H NMR (300 MHz, CDCl₃) δ (ppm) = 2.06 (s, 3 H), 2.30 (s, 3 H), 2.43-2.55 (m, 4 H), 2.62-2.72 (m, 6 H), 3.34 (t, J = 7.5 Hz, 1 H), 8.47 (bs, 1 H). **¹³C NMR** (75 MHz, CD₃OD) δ (ppm) = 22.7, 30.0, 45.9, 48.7 (2 C), 56.0 (2 C), 59.1, 156.2, 167.5. **MS** (EI) m/z 210 [M^+], 110, 99. **HRMS** (EI; [M^+]) calculated for C₁₀H₁₈N₄O 210.1481, found 210.1488.

4-(1H-Indol-3-yl)-2,6-methyl-4,5-dihydropyridazin-3(2H)-one 3i. According to the general procedure for the formation of the dihydropyridazinone cycle (method a)) starting from 100 mg of ethyl 2-(3-1H-indole)-4-oxo-pentanoate **2a** and 31 μL of methylhydrazine. The desired compound is obtained after flash column chromatography (dichloromethane/methanol gradient=9.9/0.1 to 97/3) as a yellow lacquer. Yield: 76 mg (81 %).

^1H NMR (300 MHz, CDCl_3) δ (ppm) = 2.03 (s, 3 H), 2.71-2.86 (m, 2 H), 2.41 (s, 3 H), 3.97 (t, J = 7.1 Hz, 1 H), 6.72 (dd, J = 2.4, 0.2 Hz, 1 H), 7.07-7.18 (m, 2 H), 7.24 (dd, J = 7.5, 1.5 Hz, 1 H), 7.61 (d, J = 7.8 Hz, 1 H), 8.56 (bs, 1 H). **^{13}C NMR** (75 MHz, CDCl_3) δ (ppm) = 23.5, 33.7, 34.8, 36.6, 111.6, 111.8, 119.0, 119.7, 121.8, 122.2, 126.3, 136.5, 153.7, 166.7. **IR** (KBr) ν (cm^{-1}) = à faire. **MS** (EI) m/z 241 [M^+], 212, 183, 157, 143, 129, 115. **HRMS** (EI; [M^+]) calculated for $\text{C}_{14}\text{H}_{15}\text{N}_3\text{O}$ 241.1215, found 241.1221.

Phosphodiesterase assay

PDE IV activity was monitored by using a PDE IV assay kit (Enzo) adapted to human recombinant phosphodiesterase isoform PDE IV expressed in *E. coli*. PDE I come from bovine brain and is available in PDE assay kit from Enzo. The basis for the assay is the cleavage of cAMP by the cyclic nucleotide phosphodiesterase. The 5'-nucleotide released is further cleaved by 5'-nucleotidase into the nucleoside and phosphate which is quantified using BIOMOLGREEN[®] reagent. The assay mixture (50 μL /well) contained in the assay buffer (10mM Tris-HCl, pH 7.4), PDE incubating with cAMP, 5'-nucleotidase with or without inhibitor (compounds or control) at 30°C for 60 min. The reaction was stopped by addition of 100 μL of BIOMOLGREEN[®] reagent and the plate was incubated for another 30 min to allow color to develop before reading OD on a microplate reader.

Test compounds were dissolved in DMSO with a final concentration (2%) which did not significantly affect PDE activity. A non-specific PDE inhibitor, 3-isobutyl-1-methylxanthine (IBMX) and Zardaverine as reference, were included as a test control. The initial screening on PDE IV is conducted at 500 μM . For the most potent compounds, the inhibition study on PDE IV activity included five concentrations of the drug. The IC_{50} values were evaluated by nonlinear regression and represent the mean value of two or three independent determinations, each performed in triplicate.

Molecular modeling

Protein preparation

The calculations are based on the PDB structure 1MKD (PDE4D isoform, chain A). Hydrogen atoms were added to the crystallographic structure of the protein using the xleap tool (AMBER11 package [i]). The protonation state of ionisable residues was checked using the Propka application with a focus on histidine residues coordinated to Zn²⁺ [ii]. In that case, a protonation at δ position was preferred over a protonation at the ϵ position that would generate a strong steric repulsion with the divalent cation. A previous study by Oliveira *et al.* has shown the importance of representing water molecules near the metallic centre to improve the docking performance in PDE4 [iii]. Therefore, the model was refined by adding five water molecules coordinated to Zn²⁺ (1 molecule) and Mg²⁺ (4 molecules). Also, one ion HO⁻ bridging the two metallic centers has been added. Actually, in the original PDB structure of the PDE4D-zardaverine complex, an oxygen atom is present between the divalent cations. Moreover, such a hydroxide ion has been postulated by Chen *et al.* in their study of the reaction mechanism for PDE4-catalyzed hydrolysis of cAMP [iv]. The position of these molecules was determined by using molecular mechanics relaxations (AMBER11, the force field used is parm99SB) followed by quantum chemistry relaxations (MOZYME/PM6/DH+, package MOPAC) [v]. Next, the position of all hydrogen atoms of the system was relaxed by local minimization using AMBER11.

Ligand preparation

The ligand structure was built using the Molden software [vi] and minimized using the MOPAC package (PM6/DH+ quantum mechanical level of theory) [v]. All torsional degrees of freedom were then taken into account during the docking simulations. The (*R*)- and (*S*)-enantiomers were examined.

Docking details

The Autodock Vina software was employed to investigate how the ligands bind the PDE4D protein [vii]. All torsional degrees of freedom were included during the global search. The docking was limited to a 24 Å x 40 Å x 38 Å box centered on the known binding site (as observed in the Zardaverine – PDE4D X-ray structure). Vina calculations were carried out

using the default value of 8 for the exhaustiveness parameter. No protein flexibility was considered.

NCI/IGM analysis

Additional calculations have been carried out to identify and characterize weak non-covalent interactions present in the ligand poses found by molecular docking simulations. For that, the modern tool NCI/IGM has been employed [viii,ix]. It is based on the peaks that appear at low electron density (ED) in the ED gradient drops δg plot (see references for detailed information) [viii,ix]. Here, the promolecular density (non relaxed by a quantum chemistry procedure) was used. The complementary NCI/IGM analysis was performed to confer a quantitative aspect to the parent NCI method. The δg iso-surfaces derived from these calculations provide a 3D representation of the interaction regions. In these pictures, the nature of the interaction is color-coded: blue for attractive interactions (generally hydrogen bonding), green for weakly repulsive or attractive interactions (vdW) or red for steric repulsion. The atomic scheme decomposition has been used in the present study to estimate the relative contribution of atoms in the NCI regions.

References used in the molecular modeling experimental section :

- [i] D.A. Case, T.A. Darden, T.E. Cheatham, C.L. Simmerling, J. Wang, R.E. Duke, R. Luo, R.C. Walker, W. Zhang, K.M. Merz, B. Roberts, B. Wang, S. Hayik, A. Roitberg, G. Seabra, I. Kolossváry, K.F. Wong, F. Paesani, J. Vanicek, J. Liu, X. Wu, S.R. Brozell, T. Steinbrecher, H. Gohlke, Q. Cai, X. Ye, J. Wang, M.-J. Hsieh, G. Cui, D.R. Roe, D.H. Mathews, M.G. Seetin, C. Sagui, V. Babin, T. Luchko, S. Gusarov, A. Kovalenko, P.A. Kollman, AMBER 11, University of California, San Francisco, 2010.
- [ii] M. H. M. Olsson, C. R. Søndergaard, M. Rostkowski, J. H. Jensen, *J. Chem. Theory Comput.* 7 (2011) 525-537.
- [iii] F. G. Oliveira, C. M. R. Sant'Anna, E. R. Caffarena, L. E. Dardenne, E. J. Barreiro, *Bioorg. Med. Chem.* 14 (2006) 6001-6011.
- [iv] X. Chen, X. Zhao, Y. Xiong, J. Liu, C.-G. Zhan, *J. Phys. Chem. B* 115 (2011) 12208-12219.
- [v] MOPAC2016, J. P. Stewart, Stewart Computational Chemistry, Colorado Springs, CO, USA, <http://OpenMOPAC.net> (2016).
- [vi] G. Schaftenaar, J. H. Noordik, *J. Comput. Aided Mol. Des.* 14 (2000) 123-134.
- [vii] O. Trott, A.J. Olson, *J. Comput. Chem.* 31 (2010) 455-461.
- [viii] C. Lefebvre, G. Rubez, H. Khartabil, J.-C. Boisson, J. Contreras-García, E. Hénon, *PCCP* 19 (2017) 17928-17936

[ix] E. R. Johnson, S. Keinan, P. Mori-Sánchez, J. Contreras-García, A. J. Cohen and W. Yang, *J. Am. Chem. Soc.* 132 (2010) 6498-6506.

Anti-inflammatory effects evaluation

Collection of blood samples, cell isolation and culture

Blood samples were provided from “Etablissement Français du Sang Grand Est” and were collected on EDTA (BD Vacutainer® K2E). Neutrophils were purified from whole human blood using Polymorphprep™ protocol. Contaminating red blood cells were removed by a hypotonic shock. Purified neutrophils were resuspended in RPMI 1640 Glutamax (Life Technologies) with 2.5% heat-inactivated autologous human serum and 1% PenStrep® (Life Technologies) and represented greater than 93% of the cells. PMNs were at least 93% viable. One million cells were cultured in 1 mL of complete medium for 4 h in 24-well falcon plates (Becton Dickinson) at 37°C in humidified atmosphere with 5% CO₂. The culture media consisted of medium containing 0.5% DMSO (used as a control condition) and inflammatory environment was obtain with lipopolysaccharide (LPS *E.coli* B111: O4, Sigma-Aldrich) 10 ng.mL⁻¹. PDE-IV inhibitors were added at 20 µM. At the end of the culture time, cells were centrifuged at 500 g for 10 min, supernatants were collected and frozen at -20°C.

Cell death

Cell death was determined by measuring lactate dehydrogenase (LDH) activity in cell culture supernatant according to the manufacturer’s protocol (Cytotoxicity Detection Kit (LDH) Roche). The absorbance was read at 492 nm.

IL-8 ELISA

IL-8 concentration in PMNs conditioned supernatants was measured by *Human CXCL8/IL-8 DuoSet ELISA* kit (RnD Systems) following manufacturer’s instructions. Controls included non-stimulated cells and medium alone. Levels of IL-8 were estimated using human recombinant IL-8 standard curve. The detection limit for the kit was 31,25 pg/ml.

Boyden chamber chemotaxis assay

Migration assays were performed in 48-well microchemotaxis Boyden chamber (Neuroprobe). Polycarbonate membranes with 5 µm pores were used (Nucleopore Track-etch

membrane, Whatman). Bottom wells were loaded with medium alone (negative control)] or IL-8 200 ng.mL⁻¹ (positive control for PMNs). Fifty microliters of cell suspension, treated with Zardaverin, **3a** or **3c**, were filled in upper wells at final concentration of 10⁶ cells per mL. Boyden chamber was incubated 45 min at 37°C and the lower face of the membrane was removed and stained with RAL 555 kit. The number of cells that migrated underneath the membrane was determined by counting five randomly chosen fields of microscope (Zeiss, Axiovert 200M, magnification x40).

Statistics

Each experiment was performed on cells from at least 8 independent donors. Owing to a lack of normal distribution of the assessed variables due to the small number of donors, non parametric exact Wilcoxon-Mann-Whitney tests with the *p*-value fixed at 0.05 were carried out to determine the significance of the results (StatXact7.0, Cytel Inc.).

Synthesis and Biological Evaluation of Pyridazinone derivatives as Potential Anti-inflammatory Agents

Chantal Barberot,^a Aurélie Moniot,^b Ingrid Allart-Simon,^a Laurette Malleret,^c Tatiana Yegorova,^d Marie Laronze-Cochard,^a Abderrazzaq Bentaher,^c Maurice Médebielle,^e Jean-Philippe Bouillon,^d Eric Hénon,^a Janos Sapi,^a Frédéric Velard^b and Stéphane Gérard^{*a}

Abstract : Cyclic nucleotide phosphodiesterase type 4 (PDE4), that controls intracellular level of cyclic nucleotide cAMP, has aroused scientific attention as a suitable target for anti-inflammatory therapy in respiratory diseases. Here we describe the development of two families of pyridazinone derivatives as potential PDE4 inhibitors and their evaluation as anti-inflammatory agents. Among these derivatives, 4,5-dihydropyridazinone representatives possess promising activity, selectivity towards PDE4 isoenzymes and are able to reduce IL-8 production by human primary polymorphonuclear cells.

Keywords : Pyridazinone - phosphodiesterase inhibitors - anti-inflammatory - PDE4

Highlights

- Two novel series of pyridazinones were developed for their anti-inflammatory activity.
- Molecular docking rationalized the anti-PDE4 activity.
- Compound **3c** exhibited the strongest PDE4 inhibitory activity.
- Compound **3c** was able to reduce IL-8 production.

Graphical Abstract

